

Lab on a Chip

Accepted Manuscript



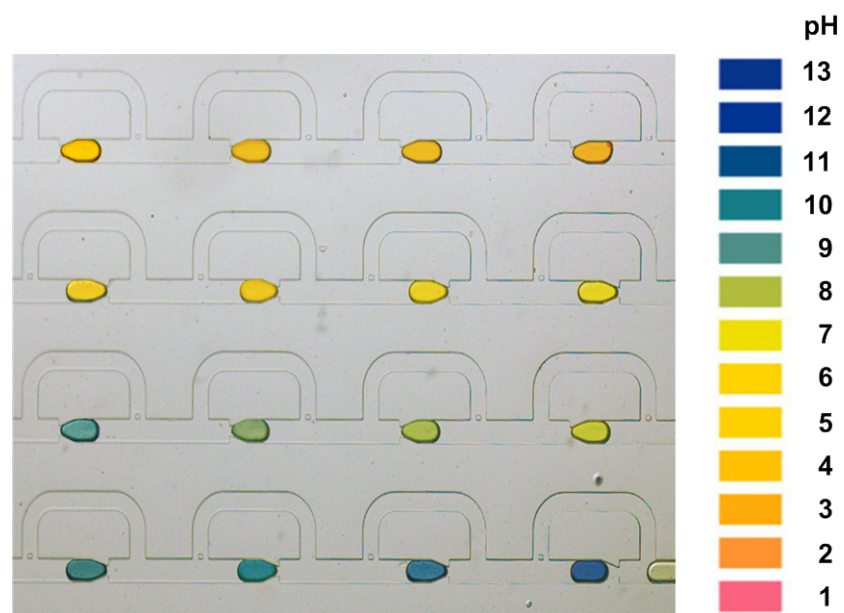
This is an *Accepted Manuscript*, which has been through the Royal Society of Chemistry peer review process and has been accepted for publication.

Accepted Manuscripts are published online shortly after acceptance, before technical editing, formatting and proof reading. Using this free service, authors can make their results available to the community, in citable form, before we publish the edited article. We will replace this *Accepted Manuscript* with the edited and formatted *Advance Article* as soon as it is available.

You can find more information about *Accepted Manuscripts* in the [Information for Authors](#).

Please note that technical editing may introduce minor changes to the text and/or graphics, which may alter content. The journal's standard [Terms & Conditions](#) and the [Ethical guidelines](#) still apply. In no event shall the Royal Society of Chemistry be held responsible for any errors or omissions in this *Accepted Manuscript* or any consequences arising from the use of any information it contains.

Stable microenvironment with pH ranging from 3 to 11 is achieved by on-demand control of droplet formation and electrolysis.



Cite this: DOI: 10.1039/c0xx00000x

www.rsc.org/xxxxxx

ARTICLE TYPE

A droplet-based pH regulator in microfluidics

Hongbo Zhou^{a,b}, Gang Li^b, and Shuhuai Yao^{*a}

Received (in XXX, XXX) Xth XXXXXXXXX 20XX, Accepted Xth XXXXXXXXX 20XX

DOI: 10.1039/b000000x

In this paper, we develop a strategy to form on-demand droplets with specific pH values. The pH control is based on electrolysis of water in microfluidics, and the produced hydrogen and hydroxyl ions are separated and confined in individual containers during the droplet generation, triggered by a pressure pulse. By tuning the applied voltages and pressure pulses, we can on-demand control the pH value in a droplet.

Introduction

pH is a measure of the hydrogen ion concentration in an aqueous solution, which determines the chemical activity or function of many molecules. Control of pH in microfluidics offers many intriguing possibilities for biological or chemical applications such as reaction¹⁻⁵ (proteolysis, protein crystallization, catalysts, etc.), separation (e.g., capillary electrophoresis⁶ and isoelectric focusing^{7,8}), cell culture⁹, and so on. Therefore, the formation of a specific pH environment is crucial in developing lab-on-a-chip devices. Conventional techniques (such as carbon dioxide dissolution^{10,11}, regulation of acid and base solutions^{12,13}) developed for pH modulation on a large scale are difficult for miniaturization and integration into microfluidics. When transferring these techniques to microfluidics, valves or membranes need to be integrated to regulate reagents flow^{9,10}. Moreover, as it takes substantial time for the bulk solutions to be well mixed, the corresponding pH regulator is neither precise nor quick in response. Using electricity to electrolyze or split water for pH control is one promising method for its easy manipulation and good compatibility with microfluidics. For water electrolysis technique^{3,14,15}, a DC voltage is applied across a pair of electrodes; H⁺ and OH⁻ ions are produced near the anode and cathode so that a stable pH gradient across the electrodes is formed. However, the concomitant products (H₂ and O₂) usually form gas bubbles and may disturb the flow in microfluidics^{2,16}. To avoid gas generation, water splitting technique, which uses electricity across a bipolar membrane to split water molecule into H⁺ and OH⁻ ions, is a superior method^{2,17}. In practical applications, the water splitting or electrolysis technology may still possess some limitations. In one aspect, the generated ions (H⁺ and OH⁻) are not in confined space. Therefore, an electric voltage need to be consistently applied to offset the diffusion and/or dispersion^{3,5,8,15}. In the other aspect, a continuous spatial gradient of pH is critical in applications where pH gradient is

needed (e.g., separation of proteins using isoelectric focusing^{7,8}), whereas other applications (such as reaction, titration, culture, etc) need a specific and stable pH in a confined environment.

Here, we propose a new droplet-based pH regulator, in which the ion products of water electrolysis are encapsulated into isolated droplets to form a stable pH environment. We first introduced its working principle, device configuration, and operation procedure. We demonstrated that the ion production and droplet size can be respectively controlled by the applied electrical and pressure pulse. Then, we performed pH characterization, and compared with the theoretical prediction. Finally, as a demonstration, we used the pH regulator to study the aggregation-induced emission (AIE) of zwitterionic hemicyanine dye, TPE-Cy, in response to acid and base conditions.

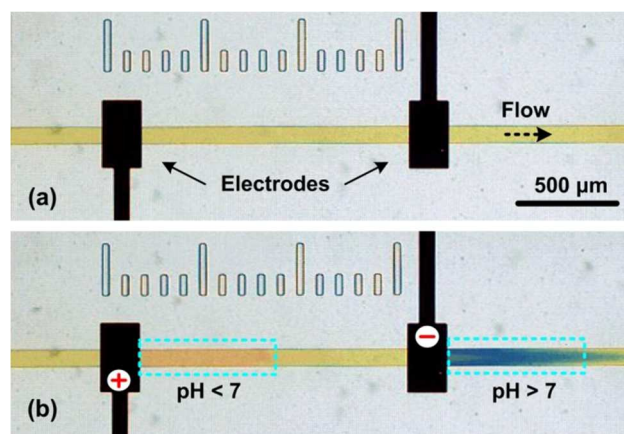
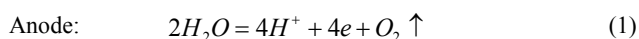


Fig 1 Illustration of conventional electrolysis-based pH regulator. In the continuous flow, pH changes in solutions near the electrodes in a microchannel (a) in the initial status and (b) upon applying a voltage. Unstable pH gradients are generated as the electrolysis products advect and/or diffuse into surroundings. The flow rate is ~0.2 mm/s, and a mixture of hydriion pH indicator solution (UI-100, Micro Essential Laboratory Inc.) and 0.1 M Na₂SO₄ solution (used as the electrolyte solution in the experiment).

Fig.1 shows the principle of a conventional pH regulator based on water electrolysis. In a microchannel, when a voltage is applied to a pair of electrodes, water is electrolyzed. H⁺ and OH⁻ ions are generated near the anode and cathode, and locally change the pH in these vicinity (Fig. 1a,b), according to^{6,7}



However, in the continuous flow, the H^+ and OH^- ions advect and

diffuse with time (Fig. 1b), which causes an unstable pH gradient and hinders forming a precise pH in close vicinity.

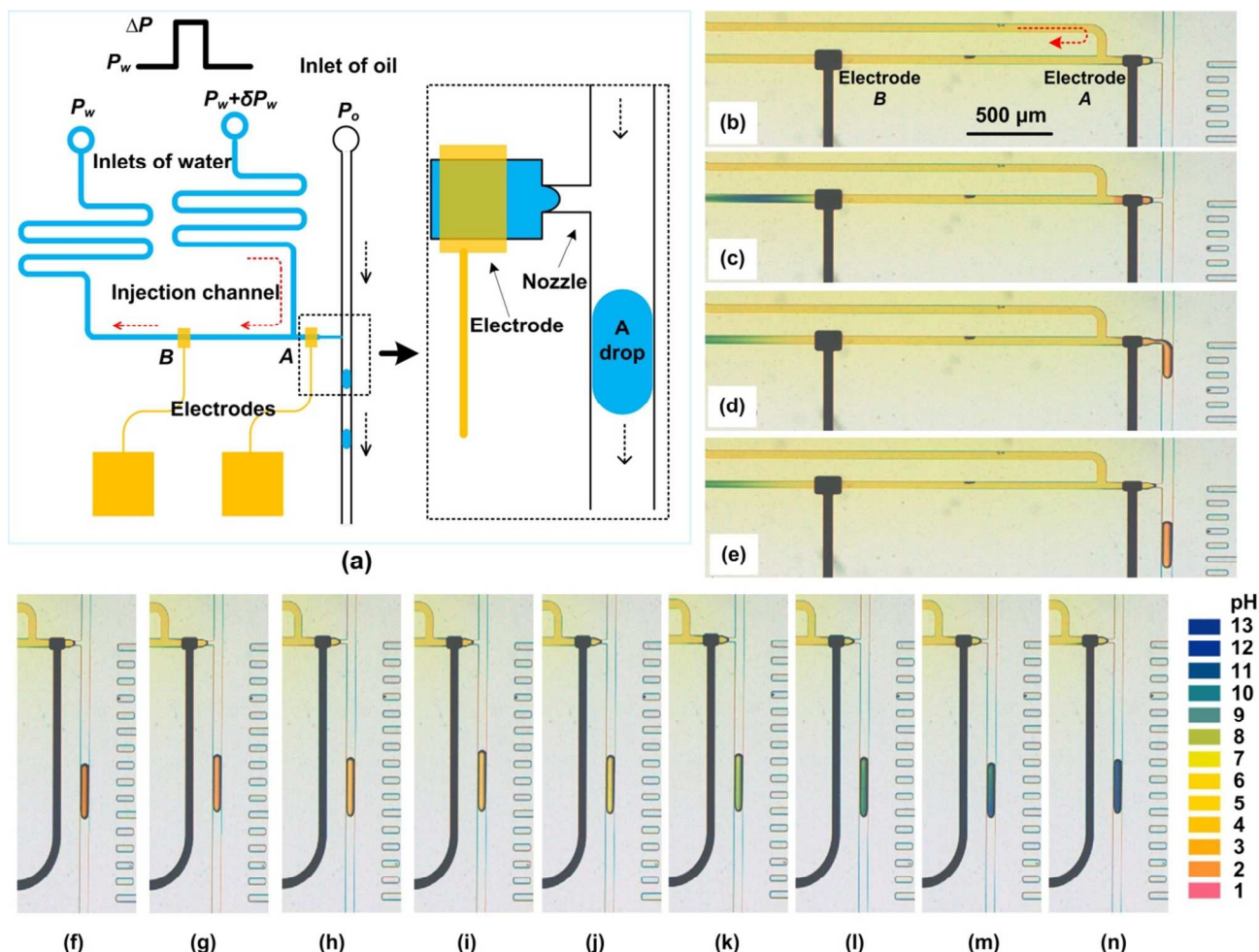


Fig. 2 The configuration and working procedure of the droplet-based pH regulator: (a) The schematic illustration of the pH regulator. The inset shows the details near the nozzle. The red and black dash arrows represent the flow directions of the oil and water phases. (b-e) The working procedure: (b) The initial status, (c) A current pulse (duration 100 ms, amplitude 5 μA) was applied to electrolyze water, (d) A pressure pulse (amplitude 1.0 psi, duration 40 ms,) was applied to inject out a droplet and (e) The recovering status. (f-n) Snapshots of the formation of pH-adjustable droplets while stepping the current pulses from +5 μA to -5 μA . A mixture of hydriion pH indicator solution (UI-100, Micro Essential Laboratory Inc.) and 0.1 M Na_2SO_4 solution was used as the electrolyte solution in the experiment.

To solve this problem, we designed a pH regulator that utilizes isolated droplets to instantaneously separate and encapsulate the electrolyzed H^+ and OH^- ions. As illustrated in Fig. 2a, the pH regulator includes an injection channel, a nozzle, a T-junction, and a pair of electrodes in the device. A pair of electrodes (for water electrolysis) is integrated in the injection channel which has two inlets. One electrode (marked as B) is located at the middle of the injection channel while the other electrode (marked as A) is located near the nozzle where the electrolysis products are encapsulated in the formed droplets. P_w and P_o are the initial pressures applied to the two water inlets and the oil inlet, respectively, to maintain a stable water/oil interface at the nozzle. An additional pressure pulse (δP_w) is imposed on the water inlet close to the nozzle to facilitate solution circulation in the injection channel. A pressure pulse (ΔP) is applied to the injection channel to trigger the formation of a droplet which contains the electrolysis ions (see details in our previous paper¹⁸).

The device consists of a poly(dimethylsiloxane) (PDMS) layer

containing microfluidic channels and a glass substrate with electrodes. The PDMS microfluidic layer was fabricated using standard soft lithography techniques. To fabricate electrodes on the glass substrate, an adhesive layer of 200 \AA Ti/W and 2000 \AA platinum were sputtered, and followed by a lift-off process. An insulation layer of silicon oxide with a thickness of 1 μm was then deposited and patterned. Finally, the PDMS replica and glass substrate were cleaned, treated with oxygen plasma, aligned under the microscope, and bonded together to seal the microchannels.

Fig. 2b-e show the working procedure of the pH regulator. The pressures applied to all the inlets are supplied by pressure transducers (2KSNNF01, Marsh Bellofram). In the experiment, the pressures P_w and P_o on the water and oil phases are 2.8 psi and 3.0 psi, respectively, which keep a stable water/oil interface near the nozzle (as shown in Fig. 2b). Meanwhile, an additional pressure δP_w (~ 0.04 psi) is applied to one water inlet (the one close to the T-junction) to circulate water flow in the injection

channel (indicated by the red dash arrows in Fig. 2a and b). When a current pulse (supplied by a source meter, Keithley 2400) is applied on the electrodes, the water is electrolyzed and H^+ and OH^- ions are generated near the anode and cathode. The ion concentration near the nozzle (H^+ ions, in the case of Fig. 2c), can be regulated by the amplitude and the duration of the current pulse. Next, a pressure pulse (amplitude 1.0 psi, duration 40 ms) imposed by a solenoid valve is applied to the two water inlets; it triggers the onset of the injection of the ions near electrode A from the nozzle. Note, the droplets volume should be large enough to encapsulate the whole produced ions near electrode A. Meanwhile, the produced ions near electrode B (OH^- ions, in the case of Fig. 2e) is washed away by the additional flow caused by δP_w . (The whole procedure can be found in Movie 1, ESI†). This flushing process is critical as it retains the same initial status. Otherwise, the ions near electrode B would accumulate and diffuse out to electrode A, which changes the ion concentrations in the background solution for predictable pH regulation. After the injection of the droplet into the oil phase (Fig. 2d), the water phase retracts to the nozzle; the system is stabilized and ready for the next cycle (Fig. 2e).

For a current pulse with duration t and constant amplitude i , in terms of Faraday's law, the ions produced by electrolysis can be calculated by integrating of the current over the total electrolysis time t^6 :

$$N = \frac{1}{nF} \int_0^t i dt = \frac{it}{nF} \quad (3)$$

where N is the number of moles of the species involved, n is the valency number of ions, and F is the Faraday constant. Considering the equilibrium of water dissociation, the pH value in a droplet with a volume V , can be expressed as:

$$pH = -\log_{10} \left(\frac{\frac{it}{nFV} + \sqrt{\left(\frac{it}{nFV}\right)^2 + 4 \times 10^{-14}}}{2} \right) \quad (4)$$

Therefore, in the experiment, by tuning the amplitude and duration of the current pulse, we can precisely tune the amount of the produced ions. Meanwhile, by tuning the amplitude and duration of the pressure pulse, we can precisely form a droplet with prescribed volume and at prescribed time¹⁸. The on-demand droplet production system has been systematically calibrated in our previous paper¹⁸. The standard deviation of the droplet size is less than 2%. In this way, a droplet with a preset pH value is formed. We kept a same pressure pulse which resulted in a constant droplet volume, ~ 1 nL, while stepping the current pulse from $-5 \mu A$ to $+5 \mu A$. As shown in Fig. 2(f-n), the pH in the droplets varies from ~ 3 to ~ 11 . This pH range is wide enough for many chemical and biological reactions.

During the electrolysis process, H_2 or O_2 are generated, accumulating in the form of gas that may significantly interfere with the flow. According to the electrolysis reactions (Eqs. (1-2)), the number of moles of produced H_2 and O_2 are half and one-fourth of the generated ions. In the experiments, the highest production of the O_2 and H_2 were estimated¹⁹ as ~ 20 pL, which were nearly two orders of magnitude lower than the droplet

volume (~ 1 nL). We expect the gas generation in our system may dissolve in the solution, therefore no bubbles were observed in the microchannels (in Fig. 2b-n).

To calibrate the performance of the pH regulator, we simply stepped the amplitude of the current pulse from 1 nA to 10 μA , and kept all the other conditions the same. For each step, thousands of droplets were generated, merged, collected, and the corresponding pH value was measured using a commercialized micro pH electrode (Lazar Research Lab, Inc). The results were plotted in Fig. 3, shown together are the model predictions (solid lines). The discrepancy between the experimental data and the model predictions, especially for the lower current amplitude, is due to the fact that only the faradaic current ($i_{faradaic}$, associated with electrolysis) should be taken into account in Eqs. (3) and (4), while the current i is composed of three parts:

$$i = i_{faradaic} + i_{charging} + i_{leakage} \quad (5)$$

where $i_{charging}$ represents the capacitive charging current to the electrode double layer capacitor (the double layer capacitance at electrode/water interface, typically $10 \sim 40 \mu F/cm^2$)²⁰ and the stray capacitors across the pair of electrodes²¹. As the RC time constant is within a few milliseconds, two orders of magnitude shorter than the current pulse duration (~ 100 ms), $i_{charging}$ takes a very small part in the total current. $i_{leakage}$ represents the leakage current to the substrates between the two electrodes. $i_{leakage}$ is estimated on the same order of the applied current i . Despite discrepancies between the model predictions and experimental data, the model (Eq. (4)) can be functioned as a guideline for pH adjustment in the droplet-based pH regulator. The calibration curve is needed for practical use.

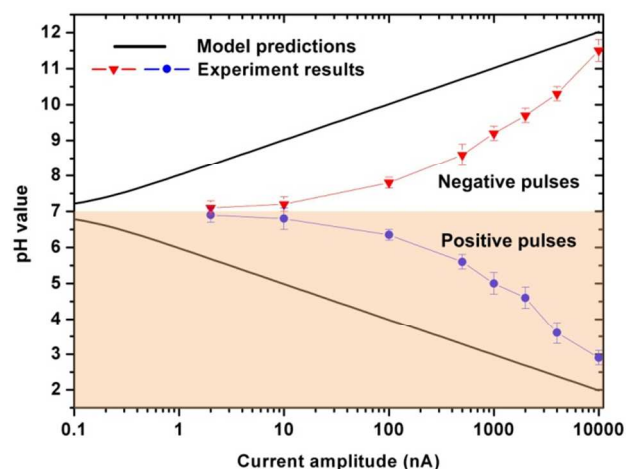


Fig. 3 The relationship between the current pulse and the pH value in the droplets. In the experiment, the current pulse duration was kept constant (100 ms), while the amplitude was changed from 1 nA to 10 μA . pH value was measured using a commercialized micro pH electrode (Lazar Research Lab, Inc) with an accuracy of 1%. The error bars represent the standard deviations for ten independent measurements. The solid lines are the model predictions based on Eq. (4).

To demonstrate the performance of the pH regulator, we performed the emission characterization of an AIE dye, TPE-Cy, at various pH values. AIE dyes exhibit significant enhancement of their light-emission in the tight packing states whereas they exhibit weak or almost no emission in loose packing state²². pH condition can affect the TPE-Cy molecular structures, change its

packing states, and then its emission intensity²³. Therefore, characterization in a series of specific and stable pH conditions is essential to screen possible pH-sensitive window and reveal the aggression characteristics of TPE-Cy in response to acid and base conditions.

Fig. 4a shows a schematic illustration of the microfluidic device. The left branch is used to form a droplet with controlled pH, while the right branch is used to form a droplet of TPE-Cy solution. In the experiments, 0.1 M Na₂SO₄ solution was used as the electrolyte solution and the concentration of TPE-Cy was chosen as 0.1 mM. Firstly, a droplet of TPE-Cy and the other droplet with controlled pH values were generated in sequence. Then, this pair of droplets was merged in a passive merging chamber^{18,24} and formed a new droplet. All the droplets had a uniform volume of 1 nL, which resulted in a series of 2 nL merged droplets. According to the calibration curve in Fig. 3, we can precisely control the pH value in the merged droplets. Figs. 4c and d show the red emission intensity of TPE-Cy versus pH

value: strong red emission at pH < 5 (region I), strong to moderate red emission at pH 5~7.5 (region II), weak to no emission at pH 7.5~11 (region III). More interestingly, there is a good linear relationship between the emission intensity and the pH in the physiological range of pH 5.5~7.5, indicating TPE-Cy is suitable to serve as a fluorescent pH-sensitive bioprobe²³. The capability of precise tune of pH allows us to investigate the molecular structures and interactions of AIE dyes at specific and stable pH conditions. Moreover, in this screening experiment, a small amount (100 μL) of TPE-Cy was used, which is especially important for testing expensive or limited samples. In combination with other microfluidic techniques, this pH regulation platform can be directly adopted in many pH-related applications, such as screening the optimum pH conditions for reactions (enzyme activities²⁵, protein crystallization²⁶ and aggregation^{23, 27}) or generating suitable pH conditions for on-chip culture²⁸.

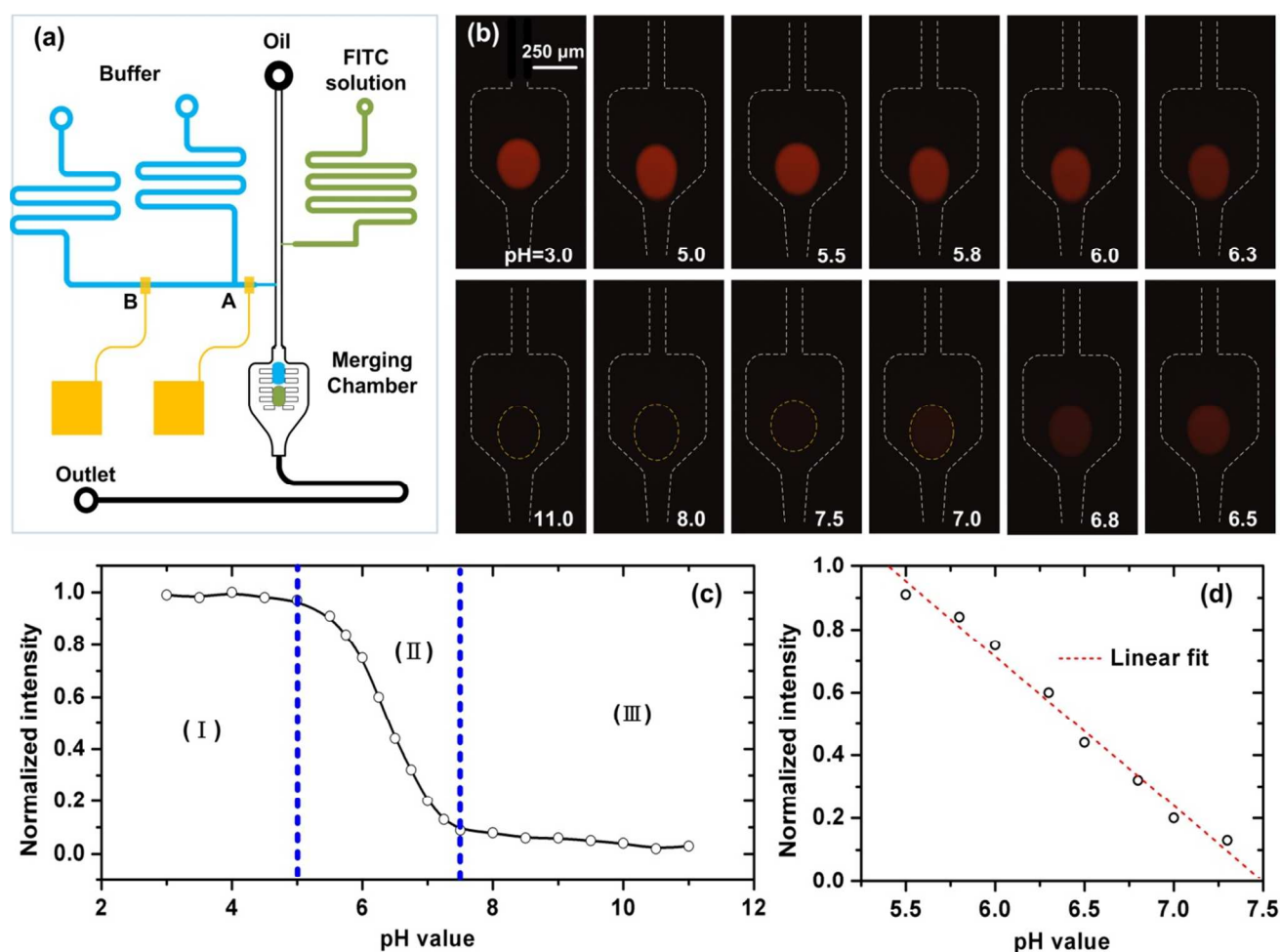


Fig.4 (a) Schematic illustration of the chip for screening the dye emission intensity vs. pH values. This chip includes two branches for generating droplets of various pH and TPE-Cy solutions, a chamber for merging droplet and a chamber array for trapping droplets. (b) The fluorescence images showing the emission intensity of the merged droplet with different pH values (ranging from 3 to 11). Imaged were taken under an inverted microscope (Eclipse Ti, Nikon) equipped with a mercury lamp and a filter cube (EX 340-380 nm; DM 400 nm; EM 605-655 nm). (c) The normalized emission intensity in the merged droplet versus pH value. There are three regions divided by the blue dash lines. (d) The details for normalized emission intensity versus pH value from 5.5 to 7.5. The red dash line is a fit of linear regression.

To our knowledge, this is the first report on a droplet-based pH regulator. By taking advantage of the compartment of droplets,

the droplet pH regulator has many inherent characters: (1) Stable. The generated ions (OH⁻ or H⁺) are separated and confined in

isolate droplets; diffusion and dispersion effects are eliminated. These stable microenvironments are essential for long-time experiments (e.g., for culture or detection). (2) Fast response. The pH value in a droplet can be changed during each cycle. The throughput of the pH regulator is a few droplets per second. Therefore, the pH values in the droplets can be on-demand changed within few seconds. (3) No bubbles formation. In the pH regulator, as the electrolysis is conducted by short pulse and the products are confined in droplets, the gas production is so low that no bubbles are detectable. Therefore, no additional functional parts (such as degassing membranes) are required. (4) Easy manipulation. The pH in a droplet can be well controlled by tuning the applied current and pressure pulses. While the existing methods need consistent electricity to maintain a stable pH value, the droplet-based pH regulator only requires an electric pulse supply during the droplet formation. (5) Compatible. In the pH regulator, the solution is handled in the format of droplets. By combining the mature techniques in droplet-based microfluidics (e.g., splitting, merging, trapping, and so on), the pH regulator can be easily applied for the pH-related on-chip reaction or detection. Moreover, sample can be transferred from the droplets to a continuous stream using a hydrophobic and oleophilic membrane or an electrical field²⁹⁻³¹ for oil removal and droplet merging.

Conclusion

In this paper, we present a simple and adaptive microfluidic system that enables on-demand formation of droplets with pH regulation in an isolated compartment. We confine the electrolysis ions into isolate droplets to avoid diffusion and dispersion effects. The pH in droplets is well controlled by tuning the applied current and pressure pulses. Compared with other methods, our droplet-based pH regulator is stable, fast in response and flexible in operation. We believe this pH regulator will find important applications in the fields such as biological assay, protein crystallization, enzyme assay, and so on.

Acknowledges

This work was supported by the Direct Allocation Grant (No. DAG12EG07-13) from HKUST and the National Science Foundation of China (No. 61006086 and 61271161). The authors thank Dr. Sijie Chen in HKUST for supplying the zwitterionic hemicyanine dye for the demonstration experiment and Dr. Lei Wu in SIMIT for her useful suggestions.

Notes and references

^a Department of Mechanical and Aerospace Engineering, Hong Kong University of Science and Technology, Hong Kong, China. Tel: 852 2358 7205; E-mail: meshyao@ust.hk
^b State Key Laboratory of Transducer Technology, Shanghai Institute of Microsystem and Information Technology, Chinese Academy of Science, China.

† Electronic Supplementary Information (ESI) available: the movie of the working procedure of the pH regulator. Two droplets with pH values of ~3 and ~11 were generated consecutively. See DOI: 10.1039/b000000x/

- 55 1. A. Aggeli, M. Bell, L. M. Carrick, C. W. Fishwick, R. Harding, P. J. Mawer, S. E. Radford, A. E. Strong and N. Boden, *Journal of the American Chemical Society*, 2003, **125**, 9619-9628.
2. L.-J. Cheng and H.-C. Chang, *Biomicrofluidics*, 2011, **5**, 046502.
3. H. J. Lee, J.-H. Kim, H. K. Lim, E. C. Cho, N. Huh, C. Ko, J. C. Park, J.-W. Choi and S. S. Lee, *Lab on a Chip*, 2010, **10**, 626-633.
4. M. Dixon, *Biochemical Journal*, 1953, **55**, 161.
5. F. Sassa, K. Morimoto, W. Satoh and H. Suzuki, *Electrophoresis*, 2008, **29**, 1787-1800.
6. H. Corstjens, H. A. Billiet, J. Frank and K. C. Luyben, *Electrophoresis*, 1996, **17**, 137-143.
7. K. Macounova, C. R. Cabrera, M. R. Holl and P. Yager, *Analytical chemistry*, 2000, **72**, 3745-3751.
8. C. R. Cabrera, B. Finlayson and P. Yager, *Analytical chemistry*, 2001, **73**, 658-666.
9. M. M. Maharbiz, W. J. Holtz, R. T. Howe and J. D. Keasling, *Biotechnology and bioengineering*, 2004, **85**, 376-381.
10. C. Läritz and L. Pagel, *Sensors and Actuators A: Physical*, 2000, **84**, 230-235.
11. Q. Zhang, S. Zeng, J. Qin and B. Lin, *Electrophoresis*, 2009, **30**, 3181-3188.
12. P. G. Righetti and A. Bossi, *Analytica chimica acta*, 1998, **372**, 1-19.
13. X. Luo, D. L. Berlin, J. Betz, G. F. Payne, W. E. Bentley and G. W. Rubloff, *Lab on a Chip*, 2010, **10**, 59-65.
14. N. M. Contento, S. P. Branagan and P. W. Bohn, *Lab on a Chip*, 2011, **11**, 3634-3641.
15. W. Wei, G. Xue and E. S. Yeung, *Analytical chemistry*, 2002, **74**, 934-940.
16. S. Z. Hua, F. Sachs, D. X. Yang and H. D. Chopra, *Analytical chemistry*, 2002, **74**, 6392-6396.
17. E. O. Gabrielsson, K. Tybrandt and M. Berggren, *Lab on a Chip*, 2012, **12**, 2507-2513.
18. H. Zhou and S. Yao, *Microfluidics and Nanofluidics*, DOI: 10.1007/s10404-013-1268-8.
19. S. Yao, D. E. Hertzog, S. Zeng, J. C. Mikkelsen Jr and J. G. Santiago, *Journal of Colloid and Interface Science*, 2003, **268**, 143-153.
20. A. J. Bard and L. R. Faulkner, *Electrochemical methods: fundamentals and applications*, Wiley New York, 2001, Chapter 1, 11-12.
21. H. Zhou and S. Yao, *Lab on a Chip*, 2013, **13**, 962-969.
22. Y. Jin, Y. Xu, Y. Liu, L. Wang, H. Jiang, X. Li and D. Cao, *Dyes and Pigments*, 2011, **90**, 311-318.
23. S. Chen, J. Liu, Y. Liu, H. Su, Y. Hong, C. K. Jim, R. T. Kwok, N. Zhao, W. Qin, J. W. Lam, S. W. Wong and B. Tang, *Chemical Science*, 2012, **3**, 1804-1809.
24. X. Niu, S. Gulati and J. B. Edel, *Lab on a Chip*, 2008, **8**, 1837-1841.
25. M.-P. N. Bui, C. A. Li, K. N. Han, J. Choo, E. K. Lee and G. H. Seong, *Analytical chemistry*, 2011, **83**, 1603-1608.
26. B. Zheng, J. D. Tice, L. S. Roach and R. F. Ismagilov, *Angewandte Chemie International Edition*, 2004, **43**, 2508-2511.
27. H. Lu, B. Xu, Y. Dong, F. Chen, Y. Li, Z. Li, J. He, H. Li and W. Tian, *Langmuir*, 2010, **26**, 6838-6844.
28. S. Köster, F. E. Angile, H. Duan, J. J. Agresti, A. Wintner, C. Schmitz, A. C. Rowat, C. A. Merten, D. Pisignano and A. D. Griffiths, *Lab on a Chip*, 2008, **8**, 1110-1115.

-
29. X. Niu, F. Pereira, J. B. Edel and A. J. de Mello, *Analytical chemistry*, 2013, **85**, 8654-8660.
30. L. M. Fidalgo, G. Whyte, D. Bratton, C. F. Kaminski, C. Abell and
5 W. T. Huck, *Angewandte Chemie International Edition*, 2008, **47**,
2042-2045.
31. G. T. Roman, M. Wang, K. N. Shultz, C. Jennings and R. T. Kennedy, *Analytical chemistry*, 2008, **80**, 8231-8238.